August, 1981] © 1981 The Chemical Society of Japan Bull. Chem. Soc. Jpn., 54, 2255—2259 (1981) 2255

Molecular Structure of Trimethylphosphine-Boron Tribromide as Determined by Gas Electron Diffraction

Kinya Iijima, Eiichi Koshimizu, and Shuzo Shibata*
Department of Chemistry, Faculty of Science, Shizuoka University, Oya, Shizuoka 422

(Received November 4, 1980)

The molecular structure of trimethylphosphine-boron tribromide $(CH_3)_3P\cdot BBr_3$ has been determined from gas electron-diffraction and vibrational-spectroscopic data. The molecular parameters and their uncertainties were r_g(B–Br)$=2.010\pm0.009$ Å, r_g(P–B)$=1.946\pm0.029$ Å, r_g(C–P)$=1.804\pm0.004$ Å, r_g(C–H)$=1.098\pm0.010$ Å, ∠BrBBr$=111.7\pm0.7°$, and ∠CPC$=108.0\pm0.7°$. The potential barrier around the P–B bond was also estimated to be about 10 kcal mol^{-1} (1 cal$=4.184$ J).

The molecular structures of trimethylamine–boron trihalides $(CH_3)_3N\cdot BX_3$ have been determined recently in both the gas and solid phases,[1–4] and the following conclusions have been drawn.[2] 1) On the formation of the complex the structural change of the acceptor molecule is greater than that of the donor molecule. 2) There is a correlation between the magnitude of the structural changes of the donor and acceptor molecules and the reorganization energy of the acceptor molecule.[5] 3) The donor-acceptor complex is stabilized and thus the N–B distance is shortened and the B–X distance is lengthened in the solid phase rather than in the gas phase.

On the other hand, the molecular structure of gaseous trimethylphosphine–boron trichloride $(CH_3)_3P\cdot BCl_3$[6] is essentially the same as that in the solid phase[7] and furthermore on the formation of the complex, the CPC angle in the donor molecule increases considerably and the C–P distance decreases, while in the case of the trimethylamine complexes the changes of the corresponding bond angle and distance are opposite. Thus it seems that trimethylphosphine and trimethylamine behave differently as a donor molecule.

In order to understand such interesting properties of trimethylphosphine donor, the structure of gaseous trimethylphosphine–boron tribromide $(CH_3)_3P\cdot BBr_3$ has been determined by an electron-diffraction method. The potential-barrier height of torsional vibration around the P–B bond has also been estimated from the combined analysis of electron-diffraction and vibrational-spectroscopic data.

Experimental

Trimethylphosphine–silver iodide complex was prepared by the procedure described in Ref. 8. The complex was decomposed under vacuum in an oil bath at 200 °C, and trimethylphosphine was collected in a trap cooled by liquid nitrogen after boron tribromide was condensed in advance. The mixture in the trap was warmed up to room temperature and was allowed to react. The crude complex obtained was recrystallized from acetone and water and was purified by repeated sublimations under vacuum.

In the electron-diffraction experiment the sample was vaporized at 200 °C by means of a high temperature nozzle. The photographs were taken using an r^3-sector on Kodak Electron-Image plates at camera distances 293.4 mm and 143.6 mm. The exposure time for the long camera distance was 17 s using an electron-beam current of 0.9 μA. For the short camera distance the exposure time was 65 s using a beam current of 0.8 μA. The pressure of the diffraction chamber was below 1×10^{-5} Torr (1 Torr$=133.3$ Pa) during the experiment. The electron wavelength was determined from the diffraction patterns of thallium chloride;[9] 0.06040 ± 0.00002 Å for the long camera distance and 0.06015 ± 0.00003 Å for the short camera distance. The optical densities of three plates taken at the long camera distance and three plates at the short camera distance were measured at 0.4 mm intervals by means of a digital microphotometer. The electron-diffraction unit and the digital microphotometer used in the present study were described in Ref. 10.

Analysis and Results

Molecular Intensity and Radial Distribution. The scattering intensites in the range of $s=2.5$—14.8 and 7.5—34.6 Å^{-1} were obtained from long and short camera distance plates, respectively. They were leveled by theoretical backgrounds, and then the intensities for each camera distance were averaged. The elastic and inelastic scattering factors were taken from the tables prepared by Schäfer *et al.*[11] and by Cromer and Mann,[12] respectively. The inelastic scattering factor for hydrogen atom was taken from the table by Tavard *et al.*[13]

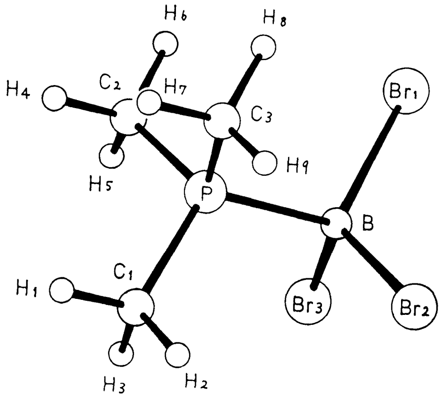

Fig. 1. Numbering of atoms in trimethylphosphine–boron tribromide (symmetry C_{3v}).

The background curves were drawn smoothly, and the molecular intensities shown in Fig. 2 were obtained.[14] Because of the large difference between the atomic numbers of bromine and other atoms in a trimethylphosphine–boron tribromide molecule, N_{ij} functions which fit μ_{ij} over the scattering-angle range for the experiment were calculated[15] and are given in Table 1. The radial distribution corrected by the N_{ij} functions is shown in Fig. 3.

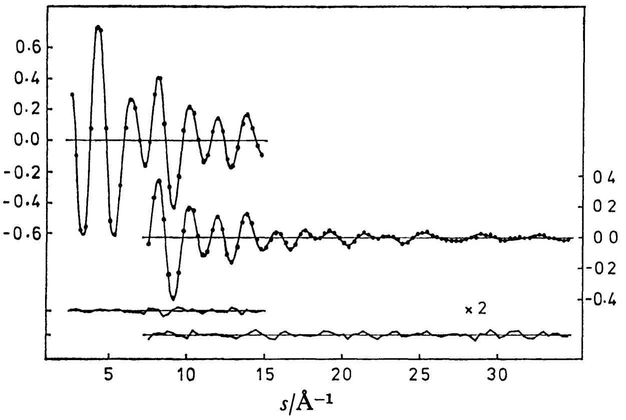

Fig. 2. Molecular intensities for trimethylphosphine–boron tribromide. The two upper curves are long and short camera-distance data. Dots represent observed ones, solid curves calculated ones, and their residuals are shown below.

TABLE 1. COEFFICIENTS OF N_{ij} FUNCTIONS

Atomic pair	a	b	c
B–Br	1.155	0.583	0.0213
B–P	1.317	1.438	0.0268
B–C	1.373	2.421	0.0222
B–H	1.485	3.227	0.0168
Br–Br	0.955	0.0	0.0
Br–P	1.080	0.0	0.0
Br–C	1.129	0.469	0.0128
Br–H	1.186	0.849	0.0070
P–C	1.282	1.133	0.0170
P–H	1.356	1.618	0.0101
C–C	1.339	2.114	0.0174
C–H	1.437	2.915	0.0136
H–H	1.529	4.014	0.0115

N_{ij} function fits μ_{ij} where $N_{ij}=a_{ij}+b_{ij}\exp(-c_{ij}s^2)$, $\mu_{ij}=|F_i|\cdot|F_j|/C_{ij}\sum(|F_k|^2+S_k)$, $C_{ij}=Z_iZ_j/\sum(Z_k^2+Z_k)$, and other notations follow Ref. 15.

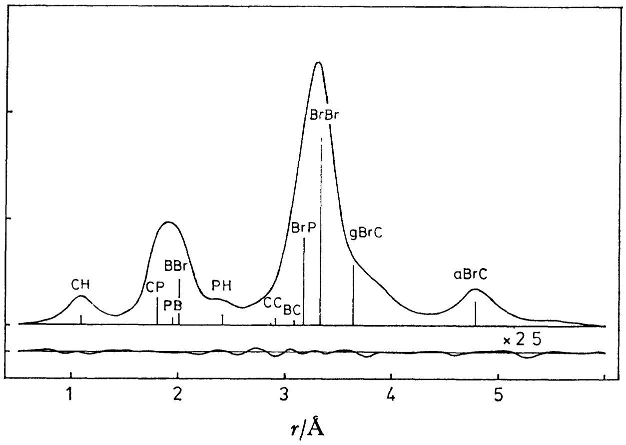

Fig. 3. Radial distribution curve for trimethylphosphine–boron tribromide. Solid curve, experimental; lower curve, 2.5 times the residuals.

Force Constant, Mean Amplitude of Vibration, and Shrinkage Effect. Drake *et al.* have studied the IR and Raman spectra of $(CH_3)_3P\cdot BBr_3$ in the solid phase and in solutions by the normal-vibration treatment.[16] We calculated the mean amplitudes of vibration, which are given in Table 5, on the basis of their force field. The calculated values for l(*gauche* Br···C), l(Br···Br), and l(B–Br), however, disagreed with the observed ones obtained from the analysis of electron-diffraction data.

The force field by Drake *et al.* was in disregard of the torsional vibrations around the P–B and C–P bonds. The torsional vibration around the P–B bond contributes significantly to l(*gauche* Br···C), and therefore the force constant of Y(P—B) was estimated so that the calculated l(*gauche* Br···C) is equal to the observed one.[1] The value obtained was 0.31×10^{-18} N m, which corresponds to the potential barrier of 9.9 kcal mol^{-1}.** The upper and lower limits of the barrier were estimated to be 18.2 and 6.7 kcal mol^{-1}, respectively. The force constant for the torsional vibration around the C–P bond was assumed to be 0.08×10^{-18} N m, which was estimated from the potential barrier for trimethylphosphine, 2.6 kcal mol^{-1}.[17] The force constants of K(B–Br) and F(Br···Br) are related mainly to l(B–Br) and l(Br···Br), respectively. These constants were also estimated as K(B–Br)$=2.0\times10^2$ N m^{-1} and F(Br···Br)$=0.30\times10^2$ N m^{-1} by the same method as used for Y(P–B).

TABLE 2. FORCE FIELD FOR $(CH_3)_3P\cdot BBr_3$

f(CH)	4.782	H(BrBBr)	0.44
f(HCH)	0.433	F(BrBr)	0.30†
f(HCP)	0.642	F(PBr)	0.25
f(CPC)	0.81	f(CH/CH′)	0.045
f(CPB)	0.84	f(HCP/HCP′)	−0.109
f(CP)	3.13	f(CP/CP′)	0.34
K(PB)	1.917	f(CPB/CPB′)	−0.06
K(BBr)	2.00†	Y(CP)	0.081†
H(PBBr)	0.42	Y(PB)	0.31†

In the present normal-coordinate calculation, general valence force constants f and Urey-Bradley force constants K, H, F, and Y were used with stretching and repulsion constants in 10^2 N m^{-1}, bending constants in 10^{-18} J rad^{-2}, and torsional constants in 10^{-18} N m. Linear constant F' was assumed as $-0.1\,F$. The values of the force constants were taken from Ref. 16, but those indicated by dagger were estimated in the present study.

The force constants of $(CH_3)_3P\cdot BBr_3$ modified in the present study are given in Table 2, and the mean amplitudes of vibration and the shrinkage effects,[18] r_a-r_α, calculated on the basis of these force constants are listed in Table 3. The force constants of K(B–Br) and F(Br···Br) obtained by Drake *et al.* (0.96 and 0.44×10^2 N m^{-1}, respectively)[16] are in disagreement with those from the present study. This may be due to the fact that the electron-diffraction experiment was carried out in the gas phase while the spectroscopic experiment was done in the solid phase and in solutions.

** The systematic error of the mean amplitude was taken into consideration because R_2 was slightly small as seen in Table 6, but it was quite small and thus the height of the potential barrier was not varied.

TABLE 3. ROOT-MEAN-SQUARE AMPLITUDES AND SHRINKAGE EFFECTS FOR $(CH_3)_3P\cdot BBr_3$ (IN 10^{-4} Å)

Atomic pair	l	r_a-r_α	Atomic pair	l	r_a-r_α
B–Br_1	596	39	P–C_1	548	194
P–B	621	18	P···H_1	1166	377
B···C_1	1059	107	C_1···C_2	1103	276
B···H_1	1268	251	C_1–H_1	783	524
B···H_2	2164	205	C_1···H_4	2236	288
Br_1···Br_2	1015	10	C_1···H_5	2283	308
Br_1···P	1061	−8	C_1···H_6	1277	506
Br_1···C_1	1079	42	H_1···H_2	1320	870
Br_1···C_2	2088	−17	H_1···H_4	3156	251
Br_1···H_1	1512	135	H_1···H_5	3577	147
Br_1···H_2	1941	128	H_1···H_6	2286	511
Br_1···H_4	2389	93	H_2···H_5	2269	551
Br_1···H_5	3433	−81	H_2···H_6	1527	670
Br_1···H_6	3152	24	H_2···H_9	3290	232

The numbering of the atoms is shown in Fig. 1. The calculated values were obtained for the same temperature (473 K) as the experiment was carried out.

Analysis of Electron Diffraction Intensities. The molecular parameters of $(CH_3)_3P\cdot BBr_3$ were determined by the least-squares analysis of molecular intensities. It was assumed that the molecule has a staggered form of C_{3v} symmetry with the methyl groups which also have C_{3v} symmetry in a staggered form with respect to the C–P bonds. The geometrical parameters determined by the least-squares analysis were as follows: r(B–Br), r(P–B), r(C–P), r(C–H), r(Br···Br), r(C···C), and ∠PCH. The mean amplitudes not listed in Table 5 and the shrinkage corrections for all the atomic pairs were fixed to the values listed in Table 3. The asymmetry parameter, κ, for the C–H bond was assumed to be 1.2×10^{-5} Å^3 by a diatomic approximation.[19] The asymmetry parameters for the other atomic pairs were ignored.

The r_α parameters determined by the least-squares calculation are listed in Table 4, where the r_g parameters and the limits of error are also listed. The random errors were given by 2.6 times the errors in least-squares calculations. The systematic errors were estimated from the errors in both the measurements of camera distance (0.04%) and wavelength (0.06%). The mean

TABLE 4. MOLECULAR PARAMETERS OBTAINED FROM LEAST-SQUARES ANALYSIS FOR $(CH_3)_3P\cdot BBr_3$

	r_α	r_g	σ[a]
B–Br	2.004	2.010	0.009
P–B	1.943	1.946	0.029
C–P	1.784	1.804	0.004
C–H	1.040	1.098	0.010
Br···Br	3.322	3.327	0.005
C···C	2.887	2.919	0.017
∠PCH	111.8		1.8
∠BrBBr[b]	112.0	111.7	0.7
∠CPC[b]	108.0	108.0	0.7

Bond distance: Å unit; bond angle: degree unit. a) Limits of error. b) Calculated from independent parameters.

TABLE 5. ROOT-MEAN-SQUARE AMPLITUDES FOR $(CH_3)_3P\cdot BBr_3$ (IN Å UNIT)

	Obsd[a]	Calcd[b]	Calcd[c]
B–Br	0.061(14)	0.060	0.073
P–B	0.035(28)	0.062	0.062
C–P	0.047(8)	0.055	0.055
C–H	0.081(12)	0.078	0.078
Br···Br	0.107(4)	0.102	0.087
Br···P	0.105(9)	0.106	0.109
anti Br···C	0.102(12)	0.108	0.113
gauche Br···C	0.207(11)	0.209	0.179
P···H	0.129(20)	0.117	0.119

a) Results obtained from the least-squares analysis of electron-diffraction data. Limits of error are shown in parentheses. b) Values calculated from the force constants in Table 2. c) Values calculated from the force constants in Ref. 16.

TABLE 6. CORRELATION MATRIX OF $(CH_3)_3P\cdot BBr_3$

	r(BBr)	r(PB)	r(CP)	r(CH)	r(BrBr)	r(CC)	∠PCH	l(BBr)	l(BrBr)	l(BrP)	l(aBrC)	l(gBrC)	l(CP)	l(PH)	l(CH)	l(PB)	R_1[a]	R_2[a]
r(BBr)	1.0																	
r(PB)	−0.97	1.0																
r(CP)	−0.49	0.55	1.0															
r(CH)	−0.04	0.05	0.00	1.0														
r(BrBr)	0.18	−0.17	−0.06	0.04	1.0													
r(CC)	−0.11	0.22	0.60	−0.01	−0.27	1.0												
∠PCH	0.07	−0.12	−0.12	−0.31	−0.27	−0.12	1.0											
l(BBr)	−0.85	0.86	0.51	0.08	−0.19	0.15	−0.01	1.0										
l(BrBr)	0.00	0.10	−0.03	0.00	−0.69	0.11	0.14	0.16	1.0									
l(BrP)	−0.29	0.30	0.08	−0.02	−0.87	0.09	0.22	0.35	0.83	1.0								
l(aBrC)	0.00	0.00	−0.07	0.05	0.02	−0.10	−0.09	0.03	0.09	0.06	1.0							
l(gBrC)	0.01	0.04	0.00	−0.10	−0.11	0.01	0.11	0.03	0.35	0.24	0.02	1.0						
l(CP)	−0.67	0.65	0.35	0.08	−0.16	−0.02	−0.03	0.74	0.16	0.32	0.08	−0.03	1.0					
l(PH)	−0.31	0.28	0.21	−0.08	−0.14	0.15	0.04	0.27	−0.01	0.13	−0.03	−0.01	0.13	1.0				
l(CH)	0.00	−0.01	−0.08	−0.08	−0.03	−0.11	0.06	0.02	0.09	0.09	0.06	0.00	0.09	−0.04	1.0			
l(PB)	−0.61	0.58	0.35	0.05	−0.14	−0.01	−0.02	0.53	0.07	0.25	0.05	−0.04	0.77	0.09	0.06	1.0		
R_1	0.07	−0.12	−0.35	0.04	−0.11	−0.64	0.12	0.03	0.39	0.36	0.19	0.00	0.21	−0.12	0.17	0.14	1.0	
R_2	0.03	−0.05	−0.20	0.00	−0.06	−0.28	−0.14	0.07	0.38	0.27	0.23	−0.08	0.27	−0.02	0.19	0.16	0.52	1.0

a) R_1 and R_2 are the indices of resolution for the long and short camera-distance data respectively. The indices of resolution and their uncertainties are $R_1=0.88\pm0.02$ and $R_2=0.80\pm0.03$.

Table 7. Comparison of molecular parameters

	$(CH_3)_3P\cdot BCl_3$		$(CH_3)_3P\cdot BBr_3$		BCl_3,[d] $(CH_3)_3P$[e]	BBr_3[f]
	Gas[a]	Solid[b]	Gas[c]	Solid[b]		
r(P–B)/Å	1.941(16)	1.957(5)	1.946(29)	1.924(12)		
r(B–X)/Å	1.851(7)	1.855(5)	2.010(9)	2.022(7)	1.742(4)	1.893(5)
r(C–P)/Å	1.800(4)	1.81(1)	1.804(4)	1.81(1)	1.846(3)	
∠XBX/°	109.4(4)	111.2(2)	111.7(7)	110.4(5)	120	120
∠CPC/°	109.3(3)	107.9(3)	108.0(7)	107.2(5)	98.6(3)	

Bond distance: Å unit; bond angle: degree unit. The values in the gas phase represent r_g parameters. a) Ref. 6. b) Ref. 7. c) Present study. d) Ref. 22. e) Ref. 20. f) Ref. 21.

amplitudes and their limits of error obtained from the least-squares analysis and the calculated mean amplitudes are listed in Table 5. The large errors in the distances and the mean amplitudes for the B–Br and P–B bonds are probably attributable to the large correlation between their parameters.

The correlation matrix is listed in Table 6, and the best-fit theoretical molecular intensities are shown in Fig. 2. The calculations of the mean amplitudes and the shrinkage effects and the least-squares analysis were carried out on a HITAC 8800/8700 computer in the Computer Center of the University of Tokyo.

Discussion

On the formation of the $(CH_3)_3P\cdot BBr_3$ complex, the B–Br distance increases by 6.2% and the BrBBr angle decreases by 6.9% (Table 7), while the C–P distance decreases by 2.3% and the CPC angle increases by 9.5%. The ratios of the changes in the B–Br and C–P distances are in good agreement with the corresponding ones in $(CH_3)_3P\cdot BCl_3$.⁶⁾ The P–B distances in both complexes are also equal to each other in the gas phases. These structural changes represent that the valence orbital of the phosphorus atom in the donor molecule changes from p^3 to sp^3 and the valence orbital of the boron atom in the acceptor molecule from sp^2 to sp^3 on the formation of a complex.

On the other hand, in the solid phase the P–B distance in $(CH_3)_3P\cdot BBr_3$ is smaller than in the gas phase with the increment of the B–Br distance and the decrement of the BrBBr angle though these changes are not large as compared with their experimental errors. This is consistent with the foregoing remarks that the force constant of K(B–Br) is larger and the F(Br···Br) is smaller in the gas phase than in the solid phase. Thus it appears that the P–B dative bond in $(CH_3)_3P\cdot BBr_3$ is enhanced in the solid phase as well as the N–B bond in $(CH_3)_3N\cdot BX_3$.

Comparing the molecular structures of trimethylphosphine-boron trihalide complexes with those of trimethylamine-boron trihalide complexes, the boron-halogen bond distances in the trimethylphosphine complexes are a little larger than those in the trimethylamine complexes ($r_g(\text{B–Cl}) = 1.836 \pm 0.002$ Å for $(CH_3)_3N\cdot BCl_3$ and $r_g(\text{B–Br}) = 2.001 \pm 0.003$ Å for $(CH_3)_3N\cdot BBr_3$).²⁾ A stronger donor gives a larger change in an acceptor molecule on the formation of a complex, and thus it seems that trimethylphosphine is a stronger donor for boron trichloride and boron tribromide than trimethylamine.

The rotational barrier around the P–B bond of $(CH_3)_3P\cdot BBr_3$ is apparently higher than that of $(CH_3)_3P\cdot BCl_3$, 3.8 ± 0.7 kcal mol^{-1}.⁶⁾ It is interesting to note that this order is inverse to the order obtained for the trimethylamine complexes, $(CH_3)_3N\cdot BCl_3$ and $(CH_3)_3N\cdot BBr_3$.²⁾ The height of the rotational barriers for these complexes may be dominated by the repulsion due to the nonbonded atomic pairs, such as $Br_1\cdots H_6$ in the case of $(CH_3)_3N\cdot BBr_3$, which have the shortest distances among the atomic pairs between the methyl groups and halogen atoms. The above order for the trimethylamine complexes will be understandable because the $Br_1\cdots H_6$ distance (2.79 Å) in $(CH_3)_3N\cdot BBr_3$ is greater than the $Cl_1\cdots H_6$ distance (2.69 Å) in $(CH_3)_3N\cdot BCl_3$. However, the order for the trimethylphosphine complexes cannot be likewise understood because the $Br_1\cdots H_6$ distance (3.25 Å) in $(CH_3)_3P\cdot BBr_3$ is nearly equal to the $Cl_1\cdots H_6$ distance (3.27 Å) in $(CH_3)_3P\cdot BCl_3$.

References

1) K. Iijima and S. Shibata, *Bull. Chem. Soc. Jpn.*, **52**, 711 (1979).

2) K. Iijima and S. Shibata, *Bull. Chem. Soc. Jpn.*, **53**, 1908 (1980).

3) S. Geller and J. L. Hoard, *Acta Crystallogr.*, **4**, 399 (1951).

4) P. H. Clippard, J. C. Hanson, and R. C. Taylor, *J. Cryst. Mol. Struct.*, **1**, 363 (1971).

5) F. A. Cotton and J. R. Leto, *J. Chem. Phys.*, **30**, 993 (1959).

6) K. Iijima and S. Shibata, *Bull. Chem. Soc. Jpn.*, **52**, 3204 (1979).

7) D. L. Black and R. C. Taylor, *Acta Crystallogr., Sect. B*, **31**, 1116 (1975).

8) R. T. Markham, E. A. Dietz, Jr., and D. R. Martin, *J. Inorg. Nucl. Chem.*, **35**, 2659 (1973).

9) W. Witt, *Z. Naturforsch., Teil A*, **19**, 1363 (1964).

10) S. Shibata, K. Iijima, R. Tani, and I. Nakamura, *Rep. Fac. Sci. Shizuoka Univ.*, **9**, 33 (1974).

11) L. Schäfer, A. C. Yates, and R. A. Bonham, *J. Chem. Phys.*, **55**, 3055 (1971).

12) D. T. Cromer and J. B. Mann, *J. Chem. Phys.*, **47**, 1892 (1967); D. T. Cromer, *ibid.*, **50**, 4857 (1969).

13) C. Tavard, D. Nicolas, and M. Rouault, *J. Chim. Phys.*, **64**, 540 (1967).

14) Numerical experimental data of the leveled total intensity and the background have been deposited with the Chemical Society of Japan (Document No. 8141).

15) K. Iijima and S. Shibata, *Bull. Chem. Soc. Jpn.*, **47**, 1393 (1974).

16) J. E. Drake, J. L. Hencher, and B. Rapp, *Inorg. Chem.*, **16**, 2289 (1977).

17) "Kagaku Binran," 2nd ed, ed by the Chemical Society of Japan, Maruzen, Tokyo (1975), p. 1330.

18) K. Kuchitsu and S. J. Cyvin, "Molecular Structures and Vibrations," ed by S. J. Cyvin, Elsevier, Amsterdam (1972), Chap. 12.

19) K. Kuchitsu, *Bull. Chem. Soc. Jpn.*, **40**, 505 (1967).

20) L. S. Bartell and L. O. Brockway, *J. Chem. Phys.*, **32**, 512 (1960).

21) S. Konaka, T. Ito, and Y. Morino, *Bull. Chem. Soc. Jpn.*, **39**, 1146 (1966).

22) S. Konaka, Y. Murata, K. Kuchitsu, and Y. Morino, *Bull. Chem. Soc. Jpn.*, **39**, 1134 (1966).